

# Photonic crystal fiber long-period gratings for biochemical sensing

**Lars Rindorf and Jesper B. Jensen**

*COM•DTU, Department of Communications, Optics and Materials, Technical University of Denmark, DK-2800 Kgs. Lyngby, Denmark*

[lhr@com.dtu.dk](mailto:lhr@com.dtu.dk)

**Martin Dufva**

*MIC•DTU, Department of Micro and Nanotechnology, Technical University of Denmark, DK-2800 Kgs. Lyngby, Denmark*

**Lars Hagsholm Pedersen and Poul Erik Høiby**

*Bioneer A/S, Kogle Alle 2, DK-2970 Hørsholm, Denmark*

**Ole Bang**

*COM•DTU, Department of Communications, Optics and Materials, Technical University of Denmark, DK-2800 Kgs. Lyngby, Denmark*

**Abstract:** We present experimental results showing that long-period gratings in photonic crystal fibers can be used as sensitive biochemical sensors. A layer of biomolecules was immobilized on the sides of the holes of the photonic crystal fiber and by observing the shift in the resonant wavelength of a long-period grating it was possible to measure the thickness of the layer. The long-period gratings were inscribed in a large-mode area silica photonic crystal fiber with a CO<sub>2</sub> laser. The thicknesses of a monolayer of poly-L-lysine and double-stranded DNA was measured using the device. We find that the grating has a sensitivity of approximately 1.4nm/1nm in terms of the shift in resonance wavelength in nm per nm thickness of biomolecule layer.

© 2006 Optical Society of America

**OCIS codes:** (060.2370) Fiber optics and optical communications, fiber optic sensors; (170.1420) Medical optics and biotechnology, biology

---

## References and links

1. K. L. Brogan and D. R. Walt, "Optical fiber-based sensors: application to chemical biology," *Current Opinion in Chemical Biology* **9**, 494–500 (2005).
2. G. Gauglitz, "Direct optical sensors: principles and selected applications," *Anal. Bioanal. Chem.* **381**, 141–155 (2005).
3. O. S. Wolfbeis, "Fiber-optic chemical sensors and biosensors," *Anal. Chem.* **76**, 3269–3283 (2004).
4. B. Lee, "Review of the present status of optical fiber sensors," *Opt. Fiber Technol.* **9**, 57–79 (2003).
5. S. W. James and R. P. Tatam, "Optical fibre long-period grating sensors: Characteristics and application," *Meas. Sci. Technol.* **14**, R49–R61 (2003).
6. M. P. DeLisa, Z. Zhang, M. Shiloach, S. Pilevar, C. C. Davis, J. S. Sirkis, , and W. E. Bentley, "Evanescence Wave Long-Period Fiber Bragg Grating as an Immobilized Antibody Biosensor," *Anal. Chem.* **72**, 2895–2900 (2000).
7. R. Slavik, J. Homola, and J. Ctyroky, "Single-mode optical fiber surface plasmon resonance sensor," *Sens. Actuators B* **54**, 74–79 (1999).
8. Y. Zhang, H. Shih, K. L. Cooper, and A. B. Wang, "Miniature fiber-optic multicavity Fabry-Perot interferometric biosensor," *Opt. Lett.* **30**, 1021–1023 (2005).
9. P. Russell, "Review: Photonic Crystal Fibers," *Science* **299**, 358–362 (2003).

10. J. C. Knight, T. A. Birks, P. S. J. Russell, and D. M. Atkin, "All-silica single-mode optical fiber with photonic crystal cladding," *Opt. Lett.* **21**, 1547–1549 (1996).
11. J. M. Fini, "Microstructure fibres for optical sensing in gases and liquids," *Meas. Sci. Technol.* **15**, 1120–1128 (2004).
12. M. A. van Eijkelenborg, M. C. J. Large, A. Argyros, J. Zagari, S. Manos, N. Issa, I. Bassett, S. Fleming, R. C. McPhedran, C. M. de Sterke, and N. A. P. Nicorovici, "Microstructured polymer optical fibre," *Opt. Express* **9**, 319 – 327 (2001).
13. F. M. Cox, A. Argyros, and M. C. J. Large, "Ultracompact biochemical sensor built with two-dimensional photonic crystal microcavity," *Opt. Express* **14**, 4135 (2006).
14. J. B. Jensen, L. H. Pedersen, P. E. Hoiby, L. B. Nielsen, T. P. Hansen, J. R. Folkenberg, J. Riishede, D. Noordegraaf, K. Nielsen, A. Carlsen, and A. Bjarklev, "Photonic crystal fiber based evanescent-wave sensor for detection of biomolecules in aqueous solutions," *Opt. Lett.* **29**, 1974–1976 (2004).
15. J. B. Jensen, P. E. Hoiby, G. Emiliyanov, O. Bang, L. H. Pedersen, and A. Bjarklev, "Selective detection of antibodies in microstructured polymer optical fibers," *Opt. Express* **13**, 5883–5889 (2005).
16. E. Chow, A. Grot, L. Mirkarimi, M. Sigalas, and G. Girolami, "Ultracompact biochemical sensor built with two-dimensional photonic crystal microcavity," *Opt. Lett.* **29**, 1093–1095 (2004).
17. T. W. Koo, S. Chan, and A. A. Berlin, "Single-molecule detection of biomolecules by surface-enhanced coherent anti-Stokes Raman scattering," *Opt. Lett.* **30**, 1024–1026 (2005).
18. R. Karlsson, A. Michaelsson, and L. Mattsson, "Kinetic-Analysis of Monoclonal Antibody-Antigen Interactions with a New Biosensor Based Analytical System," *J. Immunol. Methods* **145**, 229–240 (1991).
19. D. A. Markov, K. Swinney, and D. J. Bornhop, "Label-free molecular interaction determinations with nanoscale interferometry," *J. Am. Chem. Soc.* **126**, 16,659–16,664 (2004).
20. [Http://www.crystal-fibre.com](http://www.crystal-fibre.com).
21. G. Kakarantzas, T. A. Birks, and P. S. J. Russell, *Opt. Lett.* **27**, 1013 (2002).
22. Y. Zhu, P. Shum, J.-H. Chong, M. K. Rao, and C. Lu, "Deep-notch, ultracompact long-period grating in a large-mode-area photonic crystal fiber," *Opt. Lett.* **28**, 2467–2469 (2003).
23. P. D. Sawant, G. S. Watson, S. Myhra, and D. V. Nicolau, "Hierarchy of DNA immobilization and hybridization on poly-L-lysine using an atomic force microscopy study," *J. Nanosci. Nanotechnol.* **5**, 951–957 (2005).
24. L. Rindorf, P. E. Hoiby, J. B. Jensen, L. H. Pedersen, O. Bang, and O. Geschke, "Biomolecule detection with integrated evanescent-wave microstructured optical fibre sensor," *Anal. Bioanal. Chem.* 1–6 (Jan 2006)
25. [Http://www.nuncbrand.com](http://www.nuncbrand.com).

## 1. Introduction

Optical fibers are finding increasing application as sensors within biochemistry [1, 2, 3, 4]. In particular, long-period fiber grating sensors in conventional optical fibers have proven useful as sensors for a variety of purposes [5], including biochemical sensing [6]. Other techniques for biochemical sensing with optical fibers include surface plasmon resonance [7] and Fabry-Perot micro cavities used as an interferometric sensor [8].

Photonic crystal fibers (PCFs) [9] are optical fibers penetrated throughout their length by an array of microscopical holes. These fibers have unique light guiding properties and their array of air holes may hold a sample volume of a few nanoliters per cm of fiber. The contents of these holes, for example gases and liquids, may be probed using the evanescent-wave sensing principle [11]. PCFs are typically made from pure silica (SiO<sub>2</sub>), which is biocompatible and chemically inert. PCFs can also be made of polymer materials. Microstructured polymer optical fibers [12] are well suited for biosensing [13] since polymers allow a wide range of surface chemistries to be used.

It has been shown that photonic crystal fibers can be used for evanescent-wave sensing of biomolecules, such as DNA [14] or proteins [15]. These experiments were done using *labelled* biomolecules, where each target molecule carries a fluorescent tag. However, from a biochemical point of view, *label-free* detection of biomolecules is much more appealing, since it avoids labelling of biomolecules, which complicates the chemical process considerably and is therefore an obstacle for, e.g., designing simple-to-use point-of-care devices.

In this paper we report, to the best of our knowledge, the first *label-free* technique for detection of biomolecules using a long-period grating in a photonic crystal fiber (PCF-LPG). It is the first time long-period grating resonances have been demonstrated in a water filled photonic

crystal fiber. We demonstrate an experiment showing that the PCF-LPGs can detect the average thickness of a layer of biomolecules within a few nm. By measuring the thickness the technique may thus be used for label-free detection of selective binding of biomolecules such as DNA and proteins. The presented experiments open up new possibilities for photonic crystal fibers to be used in surface chemistry studies, such as in drug discovery and as sensors in point-of-care devices and other laboratory equipment.

Existing label-free optical detection techniques include photonic crystal slab waveguides used for biomolecule detection [16], single molecule Raman scattering [17], SPR [18], and interferometry [19].

The presented technique can not measure single-molecules, however it is robust and simple, while matching any other technique when measuring the thickness of a biofilm. It is insensitive to temperature fluctuations and does not require any calibration of the optical setup.

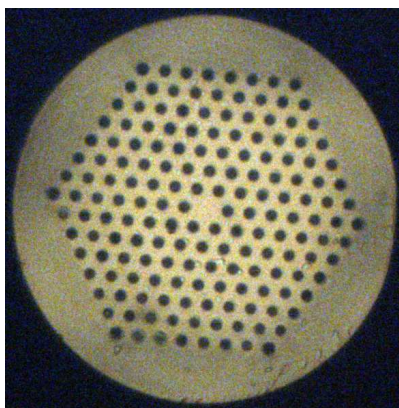


Fig. 1. End facet of the large mode area LMA10 [20] photonic crystal fiber used in the presented experiments. The fiber has the structural parameters, relative (absolute) hole size  $d/\Lambda = 0.47$  and inter-hole center distance (pitch)  $\Lambda = 7.2\mu\text{m}$ .

## 2. Photonic crystal fiber long-period gratings

We use silica photonic crystal fibers (PCFs) with a periodic triangular air hole structure and a core formed by a defect consisting of a “missing” air hole. The fibers are characterized by the relative hole size  $d/\Lambda$  and the relative free-space wavelength  $\lambda/\Lambda$ , where  $\Lambda$  is the pitch or inter-hole center distance. The end facet of the PCF used in this paper/article? is shown in Fig. 1

In an optical fiber the electrical fields can be written as  $\mathbf{E}_m(x, y, z, t) = \mathbf{E}_m(x, y)e^{i(\beta_m(\omega)z - \omega t)}$ , where  $\omega = c\frac{2\pi}{\lambda}$  is the frequency and  $\beta_m(\omega)$  is the propagation constant. The subscript  $m$  refers to the mode. The propagation constants of the modes are subjected to the dispersion relation  $\beta_m(\omega) \equiv n_m^{eff}(\omega)\frac{\omega}{c}$ , where  $n_m^{eff}(\omega)$  is the effective index of mode  $m$ . The core (*co*) and cladding (*cl*) modes have slightly different effective indices. In a PCF the lowest order mode which have the highest effective index is the two-fold degenerate core mode, which is largely confined to the core of the fiber. The higher order modes are referred to as cladding modes and their mode profiles are to a much higher extent dispersed throughout the cross section of the PCF. Cladding modes are only weakly guided in the fiber and attenuates over a couple of centimeters. If a core and a cladding mode are superposed their overall amplitude beat periodically with the so-called beat length,  $2\pi/(\beta_{co}(\omega) - \beta_{cl}(\omega))$ . The coupling of the core and cladding mode is resonant at

the wavelength where the period of the long-period grating,  $\Lambda_G$ , equals the beat length

$$\lambda = \Lambda_G \left( n_{co}^{eff}(\lambda) - n_{cl}^{eff}(\lambda) \right), \quad (1)$$

where the effective refractive indices are written as function of the free-space wavelength,  $\lambda = c \frac{2\pi}{\omega}$ .

The core mode is more confined to the silica material than the cladding mode, which has a larger portion of its field energy in the evanescent wave inside the holes of the fiber. If the refractive index of the contents of the holes is changed the effective index of the cladding mode will thus be more affected than the effective index of the core mode. This, in turn, will be seen as a shift in the resonant wavelength of the grating as this is directly dependent on the difference between the effective indices as seen in Eq. (1). The cladding modes probe all 168 holes of the PCF.

For the inscription of the long-period grating (LPG) in the PCF we use a CO<sub>2</sub> laser method [21]. The method has been demonstrated to be able to write LPGs in PCFs without any structural changes to the PCF and its holes [22].

### 3. Inscription of long-period gratings

In the experimental setup we use a Synrad Fenix CO<sub>2</sub> laser with a maximum output power of 75 W. The laser has a built-in controllable mirror, which enables us to control the movement of the laser beam very precisely. The laser has a wavelength of 10.6  $\mu\text{m}$  at which silica is completely opaque. We operate the laser at 3% power, i.e. 2.25 W. The PCF is fixed in one point in a rotational stage, which itself is mounted on a translation stage. The translational stage enables us to move the fiber with a precision less than 1  $\mu\text{m}$ . The PCF is fixed in a second point on a wheel with a groove. Both the stage and the wheel can be adjusted in height such that the PCF is in the focal point of the CO<sub>2</sub> laser. The protective polymer coating on the PCF is stripped away for a few centimeters and the bare silica surface is cleaned with methanol to remove any debris from the polymer coating. A small weight (7.11 g) is attached to the PCF with tape on the other side of the wheel to keep the fiber straight between the wheel and the stage. The rotational stage enables us to expose the fiber with the CO<sub>2</sub> laser beam from any given angle. For each grating period the fiber was sequentially exposed two times at all four sides, 0°, 90°, 180°, and 270°, since this was found to improve the quality of the grating of the dielectric change and thus removing spurious side resonances. The speed of the CO<sub>2</sub> laser beam was 2.75 mm/s exposing the PCF in 46 ms in each exposure.

We use an LMA10 fiber [20], which has a pitch of  $\Lambda = 7.2 \mu\text{m}$  and a relative (absolute) hole size of  $d/\Lambda = 0.47$ . The pitch of the PCF-LPG was chosen to  $\Lambda_G = 700 \mu\text{m}$ . The number of grating periods is chosen to be 26 making the length of grating 18.2 mm. The length of the fiber with the PCF-LPG in the middle is 30 cm in total.

### 4. Biochemistry

Poly-L-lysine is commonly used to immobilize negatively charged molecules such as DNA to a solid support. Poly-L-lysine has positively charged amino-groups that can bind to the negatively charged silica surface through an ionic binding. Poly-L-lysine will thus immobilize itself in an approximately 7 nm thick monolayer on the surface [23]. Since no additional layers can bind on the positively charged poly-L-lysine surface. DNA (deoxynucleic acid), on the other hand, has negatively charged phosphate groups in its backbone, and may thus be immobilized in a monolayer onto the poly-L-lysine, but can not bind directly onto the silica. Double-stranded DNA has an outer diameter of 2 nm and we may assume that the immobilized monolayers have

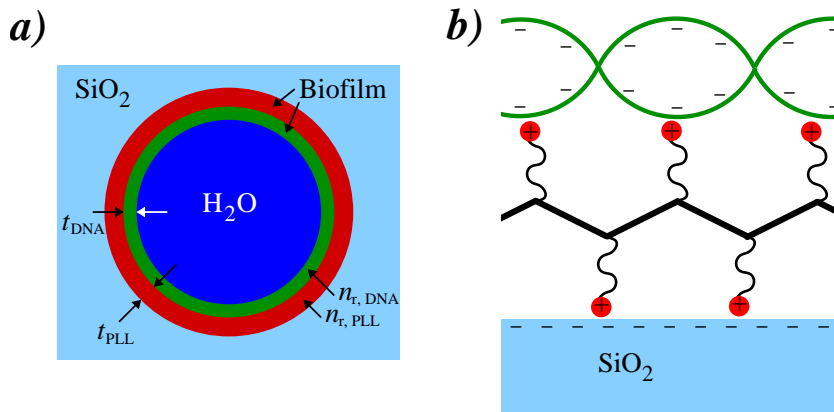


Fig. 2. (a) A hole of a photonic crystal fiber. The side is coated with poly-L-lysine (PLL) and DNA in monolayers of various thickness ( $t_{\text{DNA}}$  and  $t_{\text{PLL}}$ ) and refractive indices ( $n_{\text{r,DNA}}$  and  $n_{\text{r,PLL}}$ ). The thickness of the biofilms is vastly exaggerated compared to the hole diameter. (b) The molecular structure of poly-L-lysine (red & black) with positive charges immobilized onto the negatively charged silica surface ( $\text{SiO}_2$ ). The negatively charged DNA (green) is immobilized on the poly-L-lysine

an average thicknesses in the same magnitude when taking the orientational variations of the individual molecules into account.

The poly-L-lysine and DNA layers both have a refractive index in the order 1.45-1.48. Their refractive indices are thus closer to that of silica (1.453 at 850 nm) than that of  $\text{H}_2\text{O}$  (1.328 at 850 nm, 25°C). This is important, because if the indices were close to that of  $\text{H}_2\text{O}$ , it would be difficult, if not impossible, to detect the molecules using the evanescent wave sensing principle employed in our technique.

To introduce the solutions into the holes of the PCF we inserted one end of the PCF into a pressure chamber, which can be pressurized with an absolute pressure from around 0 to 1,100 kPa. Each sample was introduced into the PCF by a pressure drop over the fiber ends of 400 kPa. The fiber was initially washed for 30 minutes with phosphate buffered saline solution (10 mM  $\text{NaH}_2\text{PO}_4/\text{Na}_2\text{HPO}_4$  pH 7.4, 150 mM NaCl) (PBS) before being modified with poly-L-lysine (1:1000 in  $\text{H}_2\text{O}$ , w/v, Sigma #P 8920, MW=150,000-300,000). The poly-L-lysine solution was constantly flowing through the PCF for 30 minutes. The fiber was then washed in 30 minutes with PBS at 400 kPa to remove excess poly-L-lysine that had not been immobilized on the silica surface. The fiber was then removed from the pressure chamber and connected to a broadband (350-2000 nm) halogen light source (Ocean Optics HL-2000). The other end of the fiber was connected to a ANDO AQ-6315A Optical Spectrum Analyzer (450-1700 nm) set at a resolution of 2 nm. The transmission spectrum of the fiber was recorded. One end of the fiber was then inserted again into the pressure chamber. 300 base pair long double-stranded DNA (about 100 ng/uL) was introduced in the fibers for 30 minutes. The fiber was washed for 30 minutes at 400 kPa with PBS to remove any excess DNA that had not been immobilized.

## 5. Experimental results

The measured transmission spectrum of the PCF-LPG was interpolated with a polynomial of high order, which was used to find the peak of the transmission dip corresponding to the resonant wavelength of the PCF-LPG.

The PCF-LPG was tested with respect to the sensitivity of the resonant wavelength,  $\lambda_{res}$ , on temperature. With the holes of the PCF-LPG filled with air the shift of the resonant wavelength was found to be less than 2 pm/°C in the temperature interval of 23-60°C. The refractive index of air is largely independent of temperature in this interval, and we may thus conclude that the effect of thermal expansion of the PCF-LPG on the resonant wavelength due to temperature is negligible.

The refractive index of H<sub>2</sub>O is dependent on both temperature and the wavelength. A piece of fiber with a PCF-LPG was filled with demineralized H<sub>2</sub>O and mounted onto a heater stage with temperature control (MC60 & TH60, Linkam Scientific Instruments). The resonant wavelength was recorded as function of temperature and is presented in Fig. 3. In Fig. 3 we also show the temperature dependence of the refractive index of H<sub>2</sub>O,  $n_r(T, \lambda)$  at the resonant wavelength of the PCF-LPG,  $\lambda_{res}(T)$ . This is done to obtain maximal consistency when comparing the curve for the resonant wavelength with the refractive index of H<sub>2</sub>O. The dependence on temperature of the resonant wavelength of the water filled PCF-LPG is found to be -0.15 nm/°C. Figure 3 also shows the relation of the shift in resonant wavelength as function of the refractive index of the liquid, demonstrating that the PCF-LPG may also be used as a refractive index sensor.

It must be noted that the PCF-LPG responds differently to changes in the average refractive index of the liquid than to changes due to immobilization of biomolecules on the sides of the holes. We have done intensive electromagnetic field calculations to relate the shift in resonant wavelength with the thickness of the biofilm. The study is beyond the scope of this report and will be published elsewhere. The study indicates that the shift of the resonant wavelength is linear to a good approximation in the biofilm thickness until thicknesses beyond 100 nm. The linear relation is  $\Delta\lambda/\Delta t = 1.4 \text{ nm}/1.0 \text{ nm}$  in terms of the shift in resonant wavelength in nm per nm thickness biofilm, and the biofilm thus redshifts the resonant wavelength in agreement with the experimental results Fig. 4.

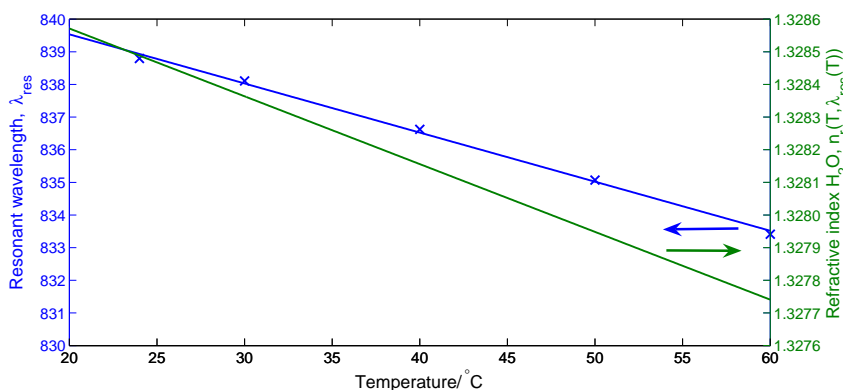


Fig. 3. The sensitivity of the water filled PCF-LPG on temperature. Experimental resonant wavelength as function of temperature (crosses) with an interpolated curve. Refractive index of water as function of temperature,  $n_r(T, \lambda_{res}(T))$

The resonant wavelength of the grating with air inside the holes was  $\lambda_{Air} = 753.6 \text{ nm}$ . The introduction of the PBS into the holes caused the resonant wavelength to shift to  $\lambda_{PBS} = 842.5 \text{ nm}$ , giving a total shift of  $\Delta\lambda = 88.9 \text{ nm}$ . The immobilization of poly-L-lysine shifts the resonant wavelength to  $\lambda_{PLL} = 849.2 \text{ nm}$ , a shift of  $\Delta\lambda_1 = 6.7 \text{ nm}$ . Finally, the DNA shifted the resonant wavelength to  $\lambda_{DNA} = 851.4 \text{ nm}$ , a shift of  $\Delta\lambda_2 = 2.3 \text{ nm}$ .

Combining the experimentally obtained wavelength shifts with the theoretically calculated coefficient described above, the average thicknesses for the poly-L-lysine and the DNA mono-

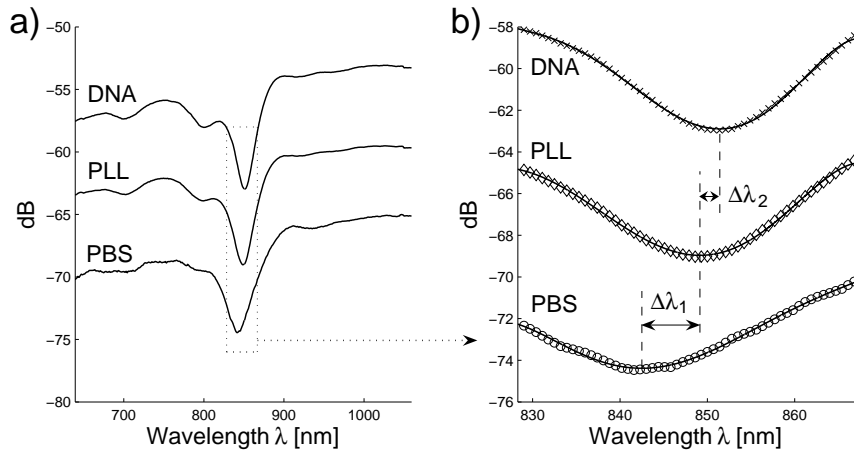


Fig. 4. (a) The experimental transmission spectra for PBS (phosphate buffered saline solution), PLL (poly-L-lysine) and double-stranded DNA. The curve for PBS shows the absolute transmission in dBm, The two other curves, PLL, DNA, are offset on the y-axis for clarity. (b) Close up of dotted rectangle in (a). The transmission spectra for PBS (circles), PLL (diamonds) and double stranded DNA (crosses). Each spectrum has been interpolated with a curve. The curve for PBS shows the absolute transmission in dBm, The two other curves, PLL, DNA, are offset on the y-axis for clarity

layers may be estimated to 4.79 nm and 1.65 nm, respectively. These values are in agreement with results obtained by atomic force microscopy, which are around 7 nm [23] for the poly-L-lysine monolayer and 2 nm for the outer diameter of the DNA double helix. Our results thus indicates that the DNA molecules have been immobilized parallel to the surface. Since the DNA molecules are 34 nm in length and 2 nm in outer diameter, they can not be expected to form a uniform monolayer of constant thickness. Rather, it would seem likely that the DNA molecules are lying flat on the surface with roughly random orientations and cross one another occasionally.

We may hypothesize that if the combined frequency shift were caused by a temperature effect, the temperature of the PCF-LPG should have decreased from room temperature to around  $-40^{\circ}\text{C}$ . We may thus exclude the possibility that the wavelength shifts are caused by temperature effects.

## 6. Discussion

The PCF-LPG sensor is reasonably sensitive for measuring refractive index with an RIU (refractive index units) of approximately  $10^{-4}$ , as seen in Fig. 3. However, the PCF-LPG does not rely on a measurement of the average refractive index of the contents of the holes. Instead the PCF-LPG is influenced significantly by the layer of biomolecules deposited on the sides of the holes, which have refractive indices close to that of silica. The evanescent wave only is most intense at the silica-water interface and vanishes completely inside the holes a short distance from this interface. This makes the sensor more robust to variations in temperature and the composition of the liquid in the air holes. It has been shown that photonic crystal fibers can be efficiently packaged in a lab-on-a-chip system [24]. The PCF-LPG biomolecule sensor may thus be implemented in a compact lab-on-a-chip system.

Following Eq. (1) the biofilm should make resonances blue shift, because the biofilm increases the effective refractive index of the cladding mode more than that of the core mode.

This is in contrast to the experimentally found results. The discrepancy can be explained when the waveguide dispersion is included in Eq. (1). This analysis, however, is beyond the scope of this work and will be presented in a separate publication.

## 7. Conclusion

We have demonstrated that long-period gratings in photonic crystal fibers can be used for sensitive biochemical sensing. An immobilized monolayer of poly-L-lysine produced a shift in resonant wavelength of the PCF-LPG of 6.7 nm and a monolayer of double-stranded DNA produced a shift in the resonant wavelength of the PCF-LPG of 2.3 nm. We estimate the immobilized poly-L-lysine layer to be 4.79 nm thick on average and the DNA monolayer to be 1.64 nm thick on average. These values agree well with the outer diameter of DNA being 2 nm and the poly-L-lysine monolayer has been measured to a thickness of around 7 nm using other techniques. The PCF-LPG has an RIU (refractive index units) sensitivity of approximately  $10^{-4}$ .

## Acknowledgments

We would like to thank the Danish ministry of Science, Technology, and Innovation (VTU, Centre Contract  $\mu$ KAP) and the Technical University of Denmark for their financial support. The authors thank Crystal Fibre A/S [20] for providing the photonic crystal fiber. NUNC A/S [25] is acknowledged for providing the CO<sub>2</sub> laser.